DOI: 10.1002/ejic.201100566

An Unusual (10,3)-d MOF Material with Nanoscale Helical Cavities and Multifunctionality

Asiata Omotayo Ibrahim,[a,b] Youfu Zhou,*[a] Feilong Jiang,[a] Lian Chen,[a] Xingjun Li,[a] Wentao Xu,[a] Oluyemi O. E. Onawumi,[b] Olusegun A. Odunola,[b] and Maochun Hong*[a]

Keywords: Metal-organic frameworks / Helical structures / Nanostructures / Nonlinear optics / Magnetic properties / Manganese / Copper / Sorption / Carbon dioxide fixation

The Mn^{II} and Cu^{II} compounds of 3-(2-pyridyl)-5,6-diphenyl-1,2,4-triazine-4,4′-disulfonic acid (H_2pdtd) were synthesized and systematically characterized. The metal-organic framework (MOF) $[Mn_2(pdtd)_2(H_2O)_4]_n{\cdot}5nH_2O$ (**1**) was constructed by a solvothermal method preformed at 140 °C with methanol as the solvent, while $[Cu(pdtd)(H_2O)_4]{\cdot}H_2O$ (**2**) was obtained by conventional solution chemistry conducted at 80 °C. Crystallographic analysis revealed that **1** has an acentric structure in which the Mn^{II} centers are linked via sulfonate groups and chelating nitrogen atoms within the pdtd ligands to give a rare noninterpenetrating (10,3)-d framework with permanent helical cavities. Consequently, **1** exhibits nonlinear optical (NLO) activity, significant CO_2 sorption, and magnetic coupling. In contrast, **2** is a mononuclear complex with coordinated water and lacks functional properties.

Introduction

The design and synthesis of MOFs[1–8] by self-assembly processes has been one of the most fascinating and challenging areas of research due to their potential application in NLO devices,[9–12] gas sorption,[13–16] magnetism,[17–20] and catalysis.[21–23] One of challenges in MOF chemistry is to construct a compound bearing various functional properties, such as MOFs with three functionalities: NLO activity, magnetism, and gas storage. One of the basic features required for NLO active materials is an acentric structure, which can potentially be induced through the introduction into the structure of an asymmetric ligand. For the construction of porous MOFs ligands with rigid units (such as phenyl and pyridyl groups) are preferable. Short and conjugated bridges within MOFs are efficient for magnetic coupling, and analogs of aromatic rings are typical conjugated groups. To achieve the goal of preparing multifunctional MOFs, a ligand containing rigid units and asymmetrically arranged O/N donors is suitable, and can be self-assembled with magnetic transition metal ions such as Mn^{II} and Cu^{II} to give the desired MOF.

In the past decades, different synthetic methods, such as hydrothermal, solvothermal, and diffusion, have been employed to build crystalline MOF materials with intriguing structures and remarkable functionalities.[24,25] The derivatives of 3-pyridyl-1,2,4-triazine have attracted much attention because of their rich coordination chemistry. For instance, 3-(2-pyridyl)-5,6-diphenyl-1,2,4-triazine yields colored complexes with some transition metal ions, which may find potential application in colorimetric analysis.[26] Other derivatives such as 2,4,6-tris[bis(pyridin-2-yl)amino]-1,3,5-triazine,[27] 2,6-bis(tetramethylfuryl)-1,2,4-triazin-3-yl)pyridine,[28] and 5,6-diphenyl-3-(2-pyridyl)-1,2,4-triazine,[29] have been employed in the construction of MOFs with different degrees of dimensionality. The analog H_2pdtd, which bears phenyl/pyridyl/triazine rings and asymmetrically arranged N/O donors, not only inherits the advantages of the 3-pyridyl-1,2,4-triazine series, but also meets the requirements for the assembly of NLO/gas storage/magnetic MOFs. It is surprising that crystalline compounds containing the pdtd ligand (where pdtd is the deprotonated form of H_2pdtd) have not been reported to date. The major difficulty lies in the fact that pdtd is a large asymmetric molecule bearing sulfonate groups that have weaker coordination abilities compared to common carboxylate groups. The solvothermal method was chosen for the preparation of these materials due to high solubility and enhanced reaction activity of the required reagents under solvothermal conditions, while a general wet chemistry method was also investigated for the purpose of comparison. MOF materials have been demonstrated to take up voluminous amounts of CO_2 and can act as CO_2 reservoirs, and as such have potential application in gas purification and CO_2 sequestration.[30,31] Taking the above into account, we investigated the self-assembly of pdtd with magnetic transition metal ions for obtaining multifunctional NLO/magnet/gas-sorption MOFs.

[a] Fujian Institute of Research on the Structure of Matter, Chinese Academy of Sciences, Fuzhou 350002, China
[b] Department of Pure and Applied Chemistry, Ladoke Akintola University of Technology, P.M.B. 4001, Ogbomoso, Nigeria

Supporting information for this article is available on the WWW under http://dx.doi.org/10.1002/ejic.201100566.

Under tailored reaction conditions, MOF **1** and the mononuclear complex **2** were obtained successfully. To the best of our knowledge, **1** is the first crystalline MOFs based on pdtd, and demonstrates NLO activity, significant CO_2 sorption and magnetic coupling. In contrast, **2** is NLO inactive and displays negligible magnetic coupling due to the isolated nature of the molecular units.

Results and Discussion

Compounds **1** and **2** were synthesized under different reaction conditions. MOF **1** was prepared via the reaction between $MnCl_2$ and pdtd by a solvothermal method (in CH_3OH at 140 °C for 3 days). Complex **2** was synthesized by a routine chemical reaction between $CuCl_2$ and pdtd in a mixture of H_2O and C_2H_5OH, and the resulting crystals were obtained through slow evaporation of the solution at room temperature. The crystallographic results revealed that compounds **1** and **2** have different structural motifs being a three-dimensional polymeric framework and a mononuclear unit, respectively. Compared to the more conventional synthesis method the solvothermal method provides better solubilities and higher reaction activities for the reagents, which overcomes the weak coordination ability of the ligand and favors the formation of a polymeric structure. Thus, the deprotonated oxygen atoms in the sulfonate groups of **1** link the metal centers in a continuous manner to form a polymeric structure. The reaction conditions for **2** are milder (80 °C) than for **1** and the resulting product is a mononuclear complex. The powder XRD patterns of **1** and **2** are consistent with the results predicted from the single crystal crystallographic data indicating that the obtained samples are phase pure (Figure S1, S2 in the Supporting Information). Furthermore, elemental analyses support the results of the powder XRD analyses, and show that the samples are chemically pure.

A Single crystal X-ray diffraction study reveals that MOF **1** crystallizes in the *Pc* space group. There are two Mn^{II} centers, two pdtd ligands, four coordinated water molecules and seven free water molecules in the asymmetric unit. The Mn1 ion is six-coordinate with distorted octahedral geometry, and is bound by four oxygen atoms from two coordinated water molecules and two sulfonate groups from two distinct pdtd ligands [Mn1–O: 2.122(8)–2.197(9) Å] and two nitrogen atoms from another pdtd ligand [Mn1–N: 2.269(7)–2.272(9) Å] (Figure 1). The sulfonate oxygen atoms are arranged in a *cis* fashion around the Mn^{II} center. The coordination sphere of Mn2 is also a distorted octahedron [Mn2–O: 2.14(1)–2.19(1) Å, Mn2–N: 2.274(8)–2.276(7) Å] and is comparable to that of Mn1. The Mn–O bond lengths are consistent with those reported for other Mn^{II} centers.[32] The deviation from normal octahedral geometry is reflected in the bond angles (°): O1–Mn1–N8, N5–Mn1–O13A, and O3–Mn1–O2 are 168.3(7), 162.5 (4), and 171.8(3), respectively.[27] It is noteworthy that the pdtd ligands in **1** are not coplanar. There are obvious twists between the triazine ring and the phenyl rings bearing the sulfonate groups, and the corresponding dihedral angles are slightly different for two the distinct pdtd ligands: 35.9 vs. 37.7° and 41.7 vs. 47.3°. Each pdtd acts as a three-connecting node through two oxygen atoms from separate sulfonate groups and one nitrogen–nitrogen chelating group created by the pyridyl and triazine rings (Scheme 1). As shown in Figure 2, five pdtd ligands are linked by Mn^{II} ions to form a ten-membered nanoscale loop (Mn1–Mn2: 9.1 Å; Mn1–Mn1C: 25.5 Å). The loops are further connected via edge-sharing to form a 3D framework with large channels that

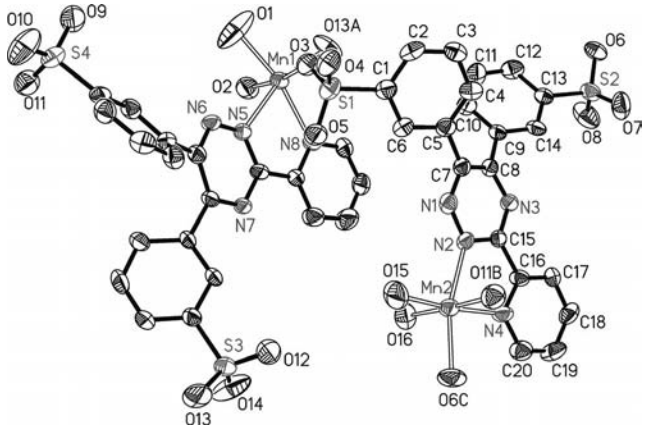

Figure 1. Coordination environment of the Mn centers in **1** (ellipsoids are drawn at the 50% probability level and the atom labeling scheme is also shown). Symmetry codes: A: *x*, –*y*, *z* – 1/2; B: *x* – 1, *y* – 1, *z*; C: *x*, –*y* – 1, *z* + 1/2.

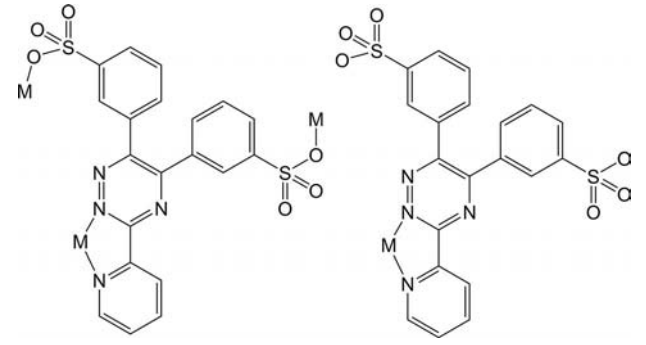

Scheme 1. Coordination modes of the pdtd ligand.

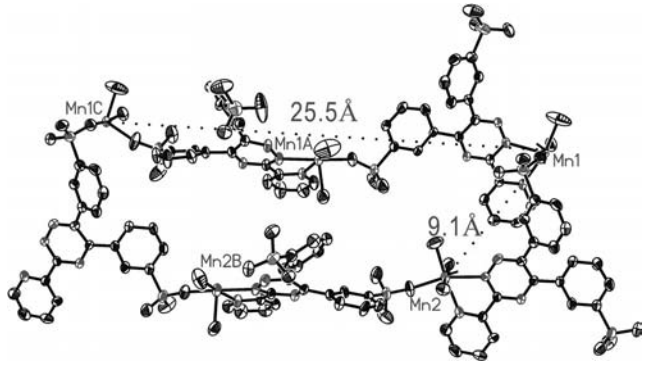

Figure 2. View of the pentanuclear loop in **1**. Symmetry codes: A: *x*, –*y*, *z* + 1/2; B: *x*, –*y* – 1, *z* + 1/2; C: *x*, *y*, *z* + 1.

run parallel to the *a* axis (Figure S3 in the Supporting Information). It is noteworthy that two uncoordinated nitrogen atoms of a trizaine group are exposed to the channels, resulting in the presence of electron-rich lone pairs inside the channels. Lattice water molecules fill the channels, and are linked to the framework by hydrogen bonding; the distance between O17 and O15 (symmetry code: $x - 1, -y - 1, z - 1/2$) is 2.91(2) Å, and the hydrogen bond angle is 100(6)°.

The structure of **2** was determined to be a mononuclear complex, and it crystallized in the $P2_1/c$ space group. As shown in Figure 3, the central Cu ion is six-coordinate, and is bound to two nitrogen atoms [Cu1–N1: 2.007(4) Å, Cu1–N4: 2.042(4) Å] from the triazine ring and pyridyl ring of a pdtd ligand and four oxygen atoms from four water molecules. Two oxygen atoms [Cu1–O9: 1.994(4) Å, Cu1–O10: 1.995(4) Å] and the two nitrogen atoms occupy the basal positions of the coordination sphere. The axial oxygen atoms [Cu1–O7: 2.328(5) Å, Cu1–O8: 2.375(4) Å] are involved in longer Cu–O bonds than the oxygen atoms in the basal positions, which results in a distorted octahedral geometry for the metal ion. The N1–Cu1–N4 angle is 80.3(2)°, which is comparable to the reported N–Cu–N angle in a complex displaying Jahn–Teller distortion.[33] The dihedral angles between the triazine ring and the phenyl rings bearing sulfonate groups are 43.3° and 42.1°. The mononuclear units are consolidated, by hydrogen bonds, to give a 3D structure (Figure S4 in the Supporting Information).

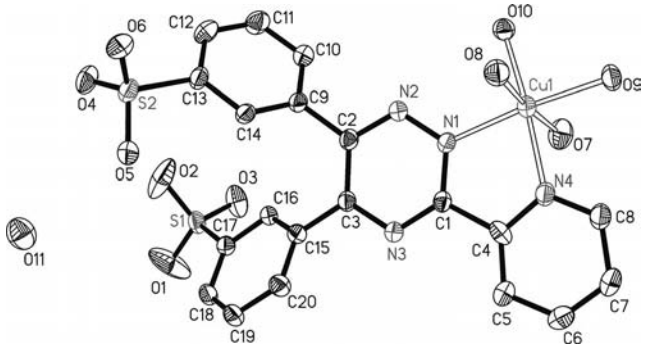

Figure 3. Asymmetric unit of **2** (ellipsoids are drawn at the 50% probability level and the atom labeling scheme is also shown).

The structure of **1** was found to be a uninodal net with a Schläfli topological term of 10^3. The net had two three-connected topologically equivalent nodes represented by the Mn^{II} ions and the averaged pdtd ligand positions. When the two coordinated water molecules are ignored, the two chelating nitrogen atoms from pdtd are reduced to a single topological link, thus the six-coordinate Mn^{II} centers become three-connecting nodes. When the structure is viewed in the *ac* plane it projects as a (6,3) net in which each helix is surrounded by six others (Figure 4). It is noteworthy that the network has both left- and right-handed helices, which alternate along the *c* axis resulting in a racemic network. Thus, the network has an extended Schläfli symbol of $10_2 \cdot 10_4 \cdot 10_4$ and is a (10,3)-d (utp) net. In addition, when viewed in the *bc* plane the structure projects as a 4×8^2 net with 4- and 8-noded helices of alternating handiness running parallel to the *c* axis, resulting in a structure comprising 2D layers and parallel helical channels. Each 4-noded helix shares common 2-nodes with a neighboring 8-noded helix to form a 10-noded circuit. The 2D layers are stacked in ABAB fashion along the *b* axis to form the resulting (10,3)-d net. One of the fantastic features in **1** is the noninterpenetrated nature of the structure. There are only four reported MOFs with noninterpenetrated (10,3)-d topologies.[34–37] Framework **1** differs from the other four (10,3)-d MOFs in the following aspects: (i) The three-connected pdtd nodes are bigger building units owing to their rigid pyridyl/triazine/phenyl rings than the nodes in the other structures, which leads to potentially larger permanent cavities; (ii) The space group of **1** is *Pc*, which is unique compared with the groups reported for the other structures ($P2_1$, $Pna2_1$); (iii) To the best of our knowledge, **1** demonstrates a (10,3)-d net with the largest helical channels (with a cross-section of about 9.1×25.5 Å^2, as shown in Figure 2) reported so far.

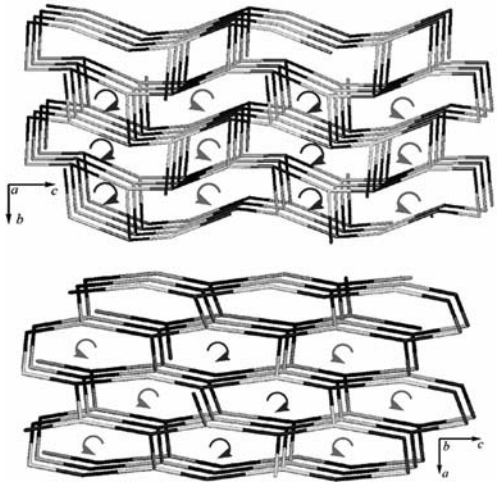

Figure 4. The utp topological net in **1** as viewed along the *a* axis (up) and the *b* axis (bottom). The Mn^{II} and pdtd nodes are shown in purple and blue, respectively.

The IR spectra of **1** and **2** exhibit strong bands at 3421 and 3396 cm^{-1}, respectively, which can be assigned to the ν(O–H) stretching of the coordinated water molecules. Weak absorption bands at 2900 and 2924 cm^{-1} in the spectra are due to the ν(C–H) vibrations of the aromatic rings of pdtd, as shown in Figure S9 in the Supporting Information. The absorption band at 2343 cm^{-1} in the spectrum of **1** is attributed to the ν(N=N) stretch (absorption by the azide group)[38] of the triazine ring of the pdtd ligand. The ν(C=N) absorption bands are observed in the spectra of compounds **1** and **2** at 1628 and 1638 cm^{-1}, respectively, and are of medium intensity. The peaks at 1121 and 1129 cm^{-1} in the spectra of **1** and **2**, respectively, are associated with the vibrations of the C–N bonds. The peaks at 1518 and 1526 cm^{-1} in the spectra of **1** and **2** are attributed to the ν(C=C) vibrations of the phenyl rings. The characteristic absorption bands of the sulfonate groups in **1** appear

at 1226, 1181, 1121 cm^{-1} for $\nu_{as}(SO_3^-)$ and 1043 cm^{-1} for $\nu_s(SO_3^-)$. Similar bands at 1217, 1188, 1119 cm^{-1} for $\nu_{as}(SO_3^-)$ and 1047 cm^{-1} for $\nu_s(SO_3^-)$ are found in the spectrum of **2**. A weak peak associated with the Mn–O bonds appears at 532 cm^{-1} in the spectrum of **1**. Weak peaks due to absorption by the Mn–N and Cu–N bonds appear at 487 and 462 cm^{-1} in the spectra for **1** and **2**, respectively. The difference between the asymmetric and symmetric sulfonate stretching wavenumbers are 183 and 170 cm^{-1} for **1** and **2**, respectively, which implies that the bonds within the monodentate and ionic sulfonate groups are comparable in strength to those within carboxylates.

Magnetic Study

To investigate the magnetic coupling ability of pdtd the temperature dependent magnetic susceptibilities of **1** and **2** were measured at 0.1 T. For **1**, the observed $\chi_m T$ value of 4.32 $cm^3\,K\,mol^{-1}$ recorded at room temperature is slightly smaller than the expected value of 4.37 $cm^3\,K\,mol^{-1}$ known for isolated Mn^{II} ions (S = 5/2) with g = 2.0. The $\chi_m T$ value undergoes a gradual decrease down to 4.27 $cm^3\,K\,mol^{-1}$ at 4 K, indicating antiferromagnetic coupling between neighboring Mn^{II} ions (see Figure S5 in the Supporting Information). It is noteworthy that the $\chi_m T$ value increases to 4.34 $cm^3\,K\,mol^{-1}$ at 2 K, implying that long-range order is present due to spin-canting or ferrimagnetic behavior.[39] The magnetic susceptibility data in the range of 20–300 K obey the Curie–Weiss law, yielding C = 4.37 $cm^3\,K\,mol^{-1}$ and θ = –0.16 K. The negative value of θ implies that there is antiferromagnetic coupling between neighboring Mn^{II} ions. To analyze the experimental data, a model incorporating isolated ions plus a molecular field was fitted to the magnetic susceptibility data, $\chi_{total} = \chi_{Mn}/[1 - (2zj' Ng^2\beta^2)\chi_{Mn}]$. The parameter zj' is based on the molecular field approximation, and is introduced to simulate the magnetic interaction between the Mn ions; all the other parameters have their usual meanings. The least-squares fitting of the model to the observed data led to g = 1.99, zj' = –0.19 cm^{-1} and $R = \Sigma(\chi T_{obsd.} - \chi T_{calcd.})^2/\Sigma(\chi T_{obsd.})^2 = 1.9 \times 10^{-4}$, values that are consistent with those for other Mn sulfonates.[40]

For **2**, the observed $\chi_M T$ vs. T curve is characteristic of a compound displaying typical paramagnetic behavior (see Figure S6). The value of $\chi_M T$ at room temperature is 0.440 $cm^3\,K\,mol^{-1}$, which is close to the expected value of 0.454 $cm^3\,K\,mol^{-1}$ known for one isolated Cu^{II} ion (S = 1/2) with g = 2.2. The value of $\chi_M T$ remains almost constant upon cooling and reaches 0.441 $cm^3\,mol^{-1}K$ at 2 K. A linear fit of the $1/\chi_M$ vs. T data gives C = 0.438 $cm^3\,K\,mol^{-1}$ and θ = 0.07 K. The negligible value of the Weiss constant also demonstrates that there is no obvious magnetic coupling between the well separated magnetic ions.[41]

CO_2 Adsorption

Thermogravimetric analyses (TGA) of compounds **1** and **2** were performed under flowing nitrogen. The curve for **1** shows two main weight loss steps (Figure 5). The first weight loss of 15.8% occurs from 30–181 °C, and corresponds to the release of lattice and coordinated water molecules from the structure (calcd. 15.7%). The second loss starts at 450 °C and reaches 42.5% at 800 °C, and can be hypothesized as corresponding to the combustion of the pdtd ligands and the collapse of the framework. To confirm the TGA results, a crystalline sample of **1** was kept in a glass container fitted with a glass stopper and heated in a tube oven under vacuum (< 10 Pa) at 400 °C for 5 h. The weight loss was measured by a METTLER XP26 microbalance and was found to be 15.9%, which is consistent with the TGA result. Powder X-ray diffraction data implied that **1** could readily be activated and maintain a crystalline framework up to 400 °C (see Figure S1). The TGA curve for **2** also exhibits two main weight loss steps (Figure 5). The release of one lattice and four coordinated water molecules from the structure occurs from 30 °C to 221 °C (calcd.: 14.5%, found: 14.4%), and combustion of the pdtd ligands occurs up to 320 °C (Figure 5).

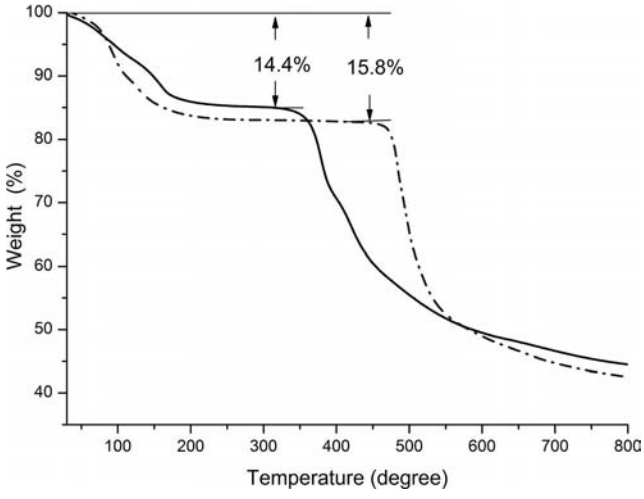

Figure 5. TGA curves for **1** (dashed line) and **2** (solid line) recorded under flowing nitrogen.

The structure of MOF **1** has large helical channels (with cross-sections of about 9.1 × 25.5 $Å^2$) and good thermal stability. PLATON calculations indicate that the crystal structure contains 15.0% of void space that is accessible to solvent molecules.[42] In addition, there are uncoordinated triazine nitrogen atoms exposed on the inside surface of the channels, which is advantageous for enhancing the CO_2 adsorption enthalpy of **1**.[14,43,44] A CO_2 adsorption isotherm was measured at 273 K for activated **1** (Figure S7). The porosity of **1** was confirmed by adsorption of CO_2, and it has an apparent Langmuir surface area of 352 $m^2\,g^{-1}$. Furthermore, the CO_2 uptake curve has a large slope, implying that **1** has a high affinity for CO_2. The amount of CO_2 adsorption at 1 atm is significant, 39.0 $cm^3\,g^{-1}$, indicating that **1** is a potential CO_2 reservoir material. The CO_2 sorption capability of **1** is comparable to that of other MOFs possessing exposed uncoordinated nitrogen atoms within their channels,[14] which enhance the CO_2 binding to the framework

by the formation of favorable interactions between the MOF and the electropositive carbons and the quadrupoles of CO_2 molecules.

NLO Property of MOF 1

1 crystallizes in the acentric space group *Pc*, Kurtz measurements were conducted to confirm the acentricity as well as to evaluate the potential application of **1** as a NLO material.[38] Preliminary results indicate that **1** displays second harmonic generation (SHG) efficiency that is approximately 1.2 times greater that that of KDP (potassium dihydrogen phosphate). The powder SHG response of **1** is modest compared to those of NLO active MOFs.[9,45–47] This may be attributed to the unfavorable arrangement of the donor-acceptor components within the pdtd ligand, which is somewhat circular in configuration, which results in weakened polarization. We have demonstrated the influence of the donor-acceptor component arrangement (parallel or antiparallel) on the NLO response of MOFs.[45] The circular configuration of **1** confirmed the effect the arrangement of an unsymmetrical ligand has upon NLO efficiency.

Conclusions

Under solvothermal conditions, the self-assembly of Mn^{II} and pdtd afforded an acentric (10,3)-d framework **1**, which is NLO-active and displays magnetic coupling. Furthermore, **1** contains nanoscale helical cavities and exhibits significant CO_2 sorption capability. In contrast, assembly conducted under milder reaction conditions yielded the mononuclear Cu^{II} complex **2**, which is centric and lacks functionality. Compound **1** is the first structurally characterized MOF containing pdtd, and exhibits potential application as a CO_2 sponge, and as a NLO and magnetic material.

Experimental Section

Materials and Methods: All chemicals were analytical grade and were used as received without further purification. Powder X-ray diffraction (PXRD) data were collected on a Rigaku MiniFlex II diffractometer. Elemental analyses were carried out on an Elemental Vario EL III microanalyzer. Infrared spectra were measured on a Perkin–Elmer Spectrum One FTIR spectrometer with KBr pellets. Thermogravimetric analyses within the 30–800 °C range were carried out with a Netzsch STA 449C Jupiter at a heating rate of 10 °C/min and with a nitrogen flow rate of 20 cm^3/min. Variable temperature magnetic measurements were conducted in an external field of 1.0 kG with a Quantum Design PPMS model 6000 magnetometer and with the samples sealed in capsules. Diamagnetic corrections were estimated with Pascal constants, and data for background corrections were obtained from experimental measurements of the sample holders. The NLO properties of the samples were measured by the Kurtz powder SHG method. The illuminating source was a Q-switched mode-locked Nd-YAG laser (λ = 1064 nm), and potassium dihydrogen phosphate (KDP) was the reference material. Adsorption isotherms were measured by a volumetric adsorption apparatus (Micromeritics' ASAP 2020 analyzer). A 35.4 mg sample was evacuated by heating at 473 K for 5 h and measurements with this sample were repeated three times.

$[Mn_2(pdtd)_2(H_2O)_4]_n \cdot 5nH_2O$ (1): A mixture of $MnCl_2 \cdot 4H_2O$ (0.119 g, 0.6 mmol), NaHpdtd (0.098 g, 0.2 mmol), and CH_3OH (10 mL) was placed in a Teflon-lined stainless steel vessel. The vessel was sealed and heated at 140 °C for 3 d, then gradually cooled to room temperature. Orange prismatic crystals of **1** were collected in 69.4% yield (0.168 g) based on NaHpdtd. $C_{40}H_{42}Mn_2N_8O_{21}S_4$ (1208.94 gmol^{-1}): calcd. C 39.74, H 3.50, N 9.27; found C 39.70, H 3.81, N 9.14. Selected IR data (KBr pellet): $\tilde{\nu}$ = 3421 (s), 2900 (w), 2343 (w), 1628 (m), 1518 (s), 1121 (m), 1181 (s), 618 (s), 532 (w), 487 (w) cm^{-1}.

$[Cu(pdtd)(H_2O)_4] \cdot H_2O$ (2): A mixture of $CuCl_2 \cdot 2H_2O$ (0.034 g, 2.0 mmol), NaHpdtd (0.246 g, 0.5 mmol), H_2O (25 mL), and C_2H_5OH (5 mL) was placed in a 50 mL Erlenmeyer flask and heated at 80 °C for 30 min. The resultant green solution was filtered and allowed to evaporate at room temperature. After one week, green prismatic crystals of **2** were collected in 45.2% yield (0.142 g) based on NaHpdtd. $C_{20}H_{22}CuN_4O_{11}S_2$ (622.08 gmol^{-1}): calcd. C 38.62, H 3.56, N 9.01; found C 38.43, H 3.57, N 8.94. Selected IR data (KBr pellet): $\tilde{\nu}$ = 3396 (s), 2924 (w), 1638 (m), 1526 (s), 1129 (m), 1188 (s), 616 (s), 462 (w) cm^{-1}.

X-Ray Crystallography: Diffraction data for compounds **1** and **2** were collected on a Rigaku Saturn 70 CCD diffractometer with Mo-K_α radiation (λ = 0.7107 Å) at 173 K and 298 K, respectively. Lorentz polarization (Lp) corrections were applied to the data. The structures were solved by direct methods and all calculations were performed with the SHELXL-97 program.[48] The metal atoms were found in the electron density map, and subsequent difference Fourier syntheses gave all the coordinates for the non-hydrogen atoms, which were then refined anisotropically. The lattice water atoms were refined isotropically. All hydrogen atoms were added to the structure with riding models and refined isotropically. Crystallographic data for **1** and **2** are summarized in Table S1 (Supporting Information), and selected bond lengths and bond angles are listed in Tables S2 and S3.

CCDC-796037 (for **1**) and -796036 (for **2**) contain the supplementary crystallographic data for this paper. These data can be obtained free of charge from The Cambridge Crystallographic Data Centre via www.ccdc.cam.ac.uk/data_request/cif.

Supporting Information (see footnote on the first page of this article): Crystallographic data (**1** and **2**), PXRD spectra, packing structures and magnetic properties for **1** and **2**, CO_2 sorption isotherm for **1**.

Acknowledgments

The authors thank the financial support by the National Natural Science Foundation of China (NSFC) (grant numbers 21071143, 91022035), the 973 Program of China, the Third World Organization for Women in Science (TWOWS) postgraduate fellowship, and the Authority of Ladoke Akintola University of Technology, Ogbomoso, Nigeria. We also thank Prof. Ding Li for the help of the Kurtz measurement.

[1] O. R. Evans, Z. Y. Wang, R. G. Xiong, B. M. Foxman, W. B. Lin, *Inorg. Chem.* **1999**, *38*, 2969.
[2] J. J. Perry, J. A. Perman, M. J. Zaworotko, *Chem. Soc. Rev.* **2009**, *38*, 1400.

[3] Q. F. Sun, J. Iwasa, D. Ogawa, Y. Ishido, S. Sato, T. Ozeki, Y. Sei, K. Yamaguchi, M. Fujita, *Science* **2010**, *328*, 1144.
[4] J. Della Rocca, W. Lin, *Eur. J. Inorg. Chem.* **2010**, 3725.
[5] C. Janiak, *Dalton Trans.* **2003**, 2781.
[6] C. Janiak, J. K. Vieth, *New J. Chem.* **2010**, *34*, 2366.
[7] R. Makiura, H. Kitagawa, *Eur. J. Inorg. Chem.* **2010**, 3715.
[8] M. Meilikhov, K. Yusenko, D. Esken, S. Turner, G. Van Tendeloo, R. A. Fischer, *Eur. J. Inorg. Chem.* **2010**, 3701.
[9] O. R. Evans, R. G. Xiong, Z. Y. Wang, G. K. Wong, W. B. Lin, *Angew. Chem.* **1999**, *111*, 557; *Angew. Chem. Int. Ed.* **1999**, *38*, 536.
[10] O. R. Evans, W. B. Lin, *Acc. Chem. Res.* **2002**, *35*, 511.
[11] Y. Kang, Y. G. Yao, Y. Y. Qin, J. Zhang, Y. B. Chen, Z. J. Li, Y. H. Wen, J. K. Cheng, R. F. Hu, *Chem. Commun.* **2004**, 1046.
[12] C. Janiak, T. G. Scharmann, P. Albrecht, F. Marlow, R. Macdonald, *J. Am. Chem. Soc.* **1996**, *118*, 6307.
[13] D. F. Sun, D. J. Collins, Y. X. Ke, J. L. Zuo, H. C. Zhou, *Chem. Eur. J.* **2006**, *12*, 3768.
[14] J. B. Lin, J. P. Zhang, X. M. Chen, *J. Am. Chem. Soc.* **2010**, *132*, 6654.
[15] A. Demessence, J. R. Long, *Chem. Eur. J.* **2010**, *16*, 5902.
[16] K. Nakagawa, D. Tanaka, S. Horike, S. Shimomura, M. Higuchi, S. Kitagawa, *Chem. Commun.* **2010**, *46*, 4258.
[17] M. Du, Y. M. Guo, S. T. Chen, X. H. Bu, S. R. Batten, J. Ribas, S. Kitagawa, *Inorg. Chem.* **2004**, *43*, 1287.
[18] X. Y. Wang, Z. M. Wang, S. Gao, *Chem. Commun.* **2008**, 281.
[19] R. Garde, C. Desplanches, A. Bleuzen, P. Veillet, M. Verdaguer, *Mol. Cryst. Liq. Cryst.* **1999**, *334*, 587.
[20] X. J. Kong, H. Zhang, H. X. Zhao, Y. P. Ren, L. S. Long, Z. P. Zheng, G. S. Nichol, R. B. Huang, L. S. Zheng, *Chem. Eur. J.* **2010**, *16*, 5292.
[21] Q. R. Fang, G. S. Zhu, M. Xue, J. Y. Sun, Y. Wei, S. L. Qiu, R. R. Xu, *Angew. Chem.* **2005**, *117*, 3913; *Angew. Chem. Int. Ed.* **2005**, *44*, 3845.
[22] Q. R. Fang, G. S. Zhu, M. Xue, J. Y. Sun, F. X. Sun, S. L. Qiu, *Inorg. Chem.* **2006**, *45*, 3582.
[23] G. Tian, G. S. Zhu, X. Y. Yang, Q. R. Fang, M. Xue, J. Y. Sun, Y. Wei, S. L. Qiu, *Chem. Commun.* **2005**, 1396.
[24] S. Kitagawa, K. Uemura, *Chem. Soc. Rev.* **2005**, *34*, 109.
[25] R. J. Hill, D. L. Long, N. R. Champness, P. Hubberstey, M. Schroder, *Acc. Chem. Res.* **2005**, *38*, 335.
[26] P. L. Croot, K. A. Hunter, *Anal. Chim. Acta* **2000**, *406*, 289.
[27] P. Gamez, P. de Hoog, O. Roubeau, M. Lutz, W. L. Driessen, A. L. Spek, J. Reedijk, *Chem. Commun.* **2002**, 1488.
[28] A. M. Fedosseev, M. S. Grigoriev, I. A. Chartishnikova, N. A. Budantseva, Z. A. Starikova, P. Moisy, *Polyhedron* **2008**, *27*, 2007.
[29] B. Machura, R. Kruszynski, J. Kusz, J. Klak, J. Mrozinski, *Polyhedron* **2007**, *26*, 4427.
[30] D. Britt, H. Furukawa, B. Wang, T. G. Glover, O. M. Yaghi, *Proc. Natl. Acad. Sci. USA* **2009**, *106*, 20637.
[31] H. Furukawa, J. Kim, N. W. Ockwig, M. O'Keeffe, O. M. Yaghi, *J. Am. Chem. Soc.* **2008**, *130*, 11650.
[32] M. C. Das, P. K. Bharadwaj, *J. Am. Chem. Soc.* **2009**, *131*, 10942.
[33] E. Tynan, P. Jensen, P. E. Kruger, A. C. Lees, M. Nieuwenhuyzen, *Dalton Trans.* **2003**, 1223.
[34] J. Zhang, Y. B. Chen, S. M. Chen, Z. J. Li, J. K. Cheng, Y. G. Yao, *Inorg. Chem.* **2006**, *45*, 3161.
[35] C. A. Black, L. R. Hanton, *Cryst. Growth Des.* **2007**, *7*, 1868.
[36] J. R. Li, Q. Yu, E. C. Sanudo, Y. Tao, X. H. Bu, *Chem. Commun.* **2007**, 2602.
[37] J. R. Li, Q. Yu, Y. Tao, X. H. Bu, J. Ribas, S. R. Batten, *Chem. Commun.* **2007**, 2290.
[38] S. K. Kurtz, *J. Appl. Phys.* **1968**, *39*, 3798.
[39] Y. Zhang, X. T. Wang, X. M. Zhang, T. F. Liu, W. G. Xu, S. Gao, *Inorg. Chem.* **2010**, *49*, 5868.
[40] F. Y. Yi, Q. P. Lin, T. H. Zhou, J. G. Mao, *Inorg. Chem.* **2010**, *49*, 3489.
[41] F. Y. Yi, Q. P. Lin, T. H. Zhou, J. G. Mao, *J. Mol. Struct.* **2010**, *984*, 416.
[42] A. L. Spek, *PLATON*, University of Utrecht, The Netherlands, **1997**.
[43] J. An, S. J. Geib, N. L. Rosi, *J. Am. Chem. Soc.* **2010**, *132*, 38.
[44] J. B. Lin, W. Xue, J. P. Zhang, X. M. Chen, *Chem. Commun.* **2011**, *47*, 926.
[45] Y. F. Zhou, D. Q. Yuan, B. L. Wu, R. H. Wang, M. C. Hong, *New J. Chem.* **2004**, *28*, 1590.
[46] J. D. Lin, X. F. Long, P. Lin, S. W. Du, *Cryst. Growth Des.* **2010**, *10*, 146.
[47] J. D. Lin, S. T. Wu, Z. H. Li, S. W. Du, *Dalton Trans.* **2010**, *39*, 10719.
[48] G. M. Sheldrick, *SHELXTL Structure Determination Software Package*, Bruker Analytical X-ray System Inc., Madison, WI, USA, **1997**.

Received: June 4, 2011
Published Online: October 11, 2011

